Snow cover response to climate change in a high alpine and half-glacierized basin in Switzerland

Jan Magnusson, Tobias Jonas, Ignacio López-Moreno and Michael Lehning

ABSTRACT

In alpine areas, the accumulation and melting of snow controls the hydrological regime. Even in watersheds where glacier melt dominates, the snow pack strongly influences the stream-flow dynamics. Prognostic simulations of the response of the snow pack to climate change were conducted in a high alpine and half-glacierized basin in central Switzerland. The snow cover and glacier were simulated using a high-resolution alpine surface model. The simulations cover a reference period (1981–2007) and two predictions (2071–2100) where the measured records of temperature, precipitation and longwave radiation were modified using six regional climate model projections for two different emission scenarios of greenhouse gases. The results show that the snow season shortens by one month at the beginning of the winter and by one and a half months at the end of the season, compared to today. The maximum snow water equivalent decreases by 27% on average. The difference in the response of the snow pack to a change in climate between the emission scenarios is rather small. The most pronounced effects of a warming climate are simulated for the highest altitudes, where all snow completely melts during summer and no snow remains for glacier accumulation.

Key words | glacier, global warming, modelling, snow cover, snow hydrology

Jan Magnusson (corresponding author)
Tobias Jonas
Michael Lehning
WSL Institute for Snow and
  Avalanche Research SLF,
Flüelastr. 11,
Davos Dorf,
Switzerland
E-mail: *magnusson@slf.ch*

Ignacio López-Moreno
Instituto Pirenaico de Ecologica, CSIC,
Campus de Aula Dei,
P.O. Box 202,
Zaragoza,
Spain

INTRODUCTION

Snow dominates the hydrological cycle in many alpine watersheds. The influence of the snow cover on the seasonal patterns of stream-flow increases with altitude. In mountain regions, the spring snowmelt is often the largest contribution to runoff throughout the year (Swift *et al.* 2005). On the other hand, discharge levels remain low during winter in snowmelt-dominated regions. On higher altitudes, the snow never melts and instead contributes to glacier regeneration. Even in watersheds where ice melt dominates the stream-flow dynamics, snowfalls on the glacier during summer increase the surface albedo. This leads to reduced melt rates with a significant effect on the temporary discharge dynamics. The meltwater from snow and ice provides water for drinking and irrigation in spring and summer. The water is often managed in reservoirs for later production of hydropower during times of increased energy demand (Schaefli *et al.* 2007). In case of global warming, the accumulation and melt of snow are expected to change and affect the hydrological regime in large parts of the world (Barnett *et al.* 2005). From the hydrological point of view, prognostic simulations of the impacts of climate change on the snow are necessary.

The depth and duration of the snow cover in the Alps depends on elevation and typical weather conditions prevailing during individual winters, and is sensitive to changes in climate (Beniston *et al.* 2003a; Laternser & Schneebeli 2003; Scherrer *et al.* 2004; Scherrer & Appenzeller 2006). The most marked changes of the snow

pack have been observed at sites on lower elevations, where relative changes are greater because of the shallow snow cover compared to the thicker snow packs at higher altitudes (Beniston 1997; Marty 2008). By combing trend analyses of historic snow measurements with predicted changes in temperature and precipitation, the duration of the seasonal snow cover is expected to shorten by about two months at the end of the 21st century in the Swiss Alps (Beniston *et al.* 2003a; Wielke *et al.* 2004). The above-mentioned findings are based on measurements on lower elevations, while conclusions regarding higher mountain ranges are more uncertain.

Model studies of the snow cover response to changes in future climate in the European Alps are mainly included in assessments of the hydrological regime shift following glacier retreat. The results are consistent and show earlier snow cover depletion, enhanced glacier retreat and that the amount and timing of basin runoff will change (Bultot *et al.* 1994; Middelkoop *et al.* 2001; Shabalova *et al.* 2003; Jasper *et al.* 2004; Huss *et al.* 2007). However, the representation of the snow cover in the models used in these studies is based on the temperature index method. This approach relies on the assumption of stationary calibration parameters, which may not be valid in the case of an increase in temperature outside of the calibration range. In this respect, energy balance models may be more reliable. However, crucial to all snow models is that they are driven with consistent input data representative of the study area, which may be a main challenge in complex alpine topography.

Simulations using energy balance models show similar trends in snow cover depletion and a shift in discharge regime for the European Alps due to global warming (Gellens *et al.* 2000; Etchevers *et al.* 2002; Beniston *et al.* 2003b; Keller *et al.* 2005; Bavay *et al.* 2009). These studies focus on large watersheds mainly without glaciers where temperatures are relatively warm compared to the higher regions in the Alps. For cold regions climate change may even lead to faster snow accumulation because of an expected increase in precipitation during winter, contradicting the above-mentioned findings (Hosaka *et al.* 2005; Raisanen 2008). The energy balance models used in previous studies often have a limited representation of the effect of the mountainous terrain on snowmelt. Snow cover is represented on a single-layer basis, and therefore

with a rather simple representation of the energy budget. In spite of the existing studies dealing with the snow cover response to climate change in the Alps, many important regions have not yet been investigated with appropriate model simulations.

This paper examines the snow cover response to climate change in a high alpine and half-glaciated watershed where the hydrological regime is dominated by the accumulation and melting of snow and the glacier itself. The snow cover, in combination with the underlying glacier ice, was simulated with the physically based and spatially distributed model Alpine3D (Lehning *et al.* 2006). The simulation covers almost 30 years with meteorological measurements from 1981 to 2007. Measurements of temperature, precipitation and radiation were modified using a statistical downscaling method to simulate the snow cover characteristics expected by the end of the 21st century, according to projections by six different regional climate models (RCMs).

Study area

The Damma glacier basin, northerly of the main Alp ridge in central Switzerland (N 46°38.177′, E 08°27.677′) has an area of $12\,km^2$ and elevations from 1,844 to 3,621 m a s l (Figure 1). The weather is mainly influenced from the north as the main ridge of the Alps in the south acts as a climate barrier. The runoff from the basin discharges entirely to a hydropower dam (Göscheneralpsee). Measurements of the glacier extension started in 1921 and since then the glacier front has retreated by about 10 m per year (Hammerli *et al.* 2007). An advance of the glacier front was recorded between 1972 and 1991. Today, the glacier occupies about $5\,km^2$ of the total basin area. The catchment is underlain by granite bedrock and glacier tills are to be found on the land, which until recently was covered by the glacier.

DATA AND METHODS

Model description

Alpine3D is a spatially distributed model based on the physical behaviour of snow and is designed for high-resolution simulations of mountain surface processes in
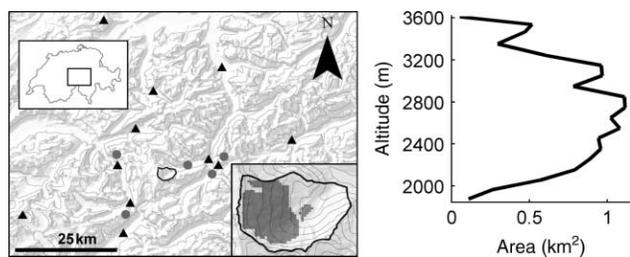
Figure 1 | Left panel: Map of Damma glacier watershed (polygon in center of image) and surrounding area, location of weather stations (black triangles) and snow stations (grey circles). The area shown in the map is located in central Switzerland (upper left inset). The glaciated areas within the watershed are shaded (close-up in lower right inset). Right panel: Distribution of elevation within the watershed.

alpine terrain (Lehning *et al.* 2006). The snow pack is modelled by solving the heat and mass transfer equations of the snow cover. Simulations of the snow microstructure development within each layer of the snow pack determine the thermal conductivity and viscosity (Lehning *et al.* 2002). As a stand-alone application, the snow module (SNOW-PACK) has previously been used for climate change impacts research (Rasmus *et al.* 2004) and is also capable of representing phase changes and densification from snow to ice. It can therefore be used for simulating glacier development and the transformation between snow and ice (Obleitner & Lehning 2004; Michlmayr *et al.* 2007). The radiation distribution in the basin is described by a view-factor approach while solar shadowing, reflections and long-wave irradiance by surrounding terrain are included in the energy balance (Fierz *et al.* 2003).

Alpine3D is initialized with a grid-based digital elevation model (100 m resolution) and a description of the soil properties on the same lattice. The simulations are driven by hourly meteorological measurements or predictions of air temperature, relative humidity, wind speed, precipitation and incoming long- and shortwave radiation. Data are provided by several surrounding automatic weather stations (details below). Precipitation is measured by heated gauges where, for each grid cell, the model determines whether precipitation falls as rain or snow by means of the local air temperature.

Description of the model simulations

Three model simulations were completed for this study. In a first simulation, the present snow cover was modelled.

The model was initialized with the glacier extent of the year 2000. The change in glacier extent within the simulation period was considered negligible because it only affected a few grid cells around the glacier tongue. In two further simulations, the snow cover at the end of the 21st century was modelled. These simulations were initialized without the glacier as studies predict that glaciers of similar size and at similar altitude ranges are expected to have completely melted due to global warming by then (Horton *et al.* 2006; Zemp *et al.* 2006). The focus of this study is on the dynamics of the seasonal snow cover. Ice and firn underlying the snow profiles were therefore removed in a post-processing step (firn was defined as snow older than one year).

In the first simulation, the present conditions were modelled using unmodified regional meteorological measurements from 1981 to 2007. In the two prediction simulations of the future, the snow cover conditions were modelled for the period 2071–2100 for two different emission scenarios of greenhouse gases. The two different emission scenarios were the Special Report on Emission Scenarios (SRES) A2 and B2 scenarios defined by the Intergovernmental Panel on Climate Change (IPCC) (Nakicenovic *et al.* 1998). Scenario A2 predicts a strong increase of carbon dioxide in the atmosphere, whereas scenario B2 predicts a moderate increase of greenhouse gases. For both prediction simulations, the observed regional meteorological measurements from 1981 to 2007 were modified to be representative of the future period based on the differences between the control and scenario runs of an ensemble of RCM simulations (for details see section 'Model input: Modifying regional measurements to future conditions').

Finally, as input for the three simulations, the observed and the modified measurement series were distributed to the model grid either by interpolation as a pre-processing step or by the radiation module of Alpine3D (see following section for details).

Model input: distributing regional measurements to the watershed

Hourly measurements (observed or modified to future conditions) from eleven stations surrounding the basin were used to drive the model. These stations are located at a distance of 10–41 km away from the study area,

and represent an altitude range 451–3,580 m a s l (Figure 1). Temperature, humidity, wind speed and precipitation input data were distributed to the model grid using the interpolation methods of Zappa et al. (2005) for meteorological data. For these parameters, inverse distance weighting was selected as an interpolation method (Shepard 1968) in combination with elevation-dependent detrending. However, radiation measurements were distributed within the watershed by the complex-terrain radiation module of Alpine3D (Fierz et al. 2003). Hourly measurements of incoming shortwave radiation were acquired at a station 12 km away from the basin. Longwave radiation has not been measured in the vicinity, but was modelled from temperature, relative humidity and sunshine duration data (from the same station that provided shortwave radiation data) using methods given by Pirazzini et al. (2000). Pirazzini derived the incoming longwave radiation by applying the Stefan-Boltzmann equation using measured air temperature and an estimate of the atmospheric emissivity. The clear sky emissivity was described as a function of air temperature and water vapour pressure, the latter estimated from measurements of relative humidity and air temperature. Pirazzini included a correction factor to adjust for the increase in emissivity of a clouded sky.

Model input: modifying regional measurements to future conditions

To generate meteorological conditions representative of possible future climate characteristics, changes in temperature, precipitation and incoming longwave radiation were taken into account. These parameters were expected to have the greatest influence on the seasonal snow pack development. To estimate possible future climate conditions, RCM simulations were used (Christensen et al. 2007) of daily minimum and maximum temperatures, daily accumulated precipitation and daily averages of incoming longwave radiation. These simulations were available for a control period (1961–1990) and for a future period (2071–2100) with a spatial resolution of 50 km on the public PRUDENCE data archive (http://prudence.dmi.dk).

Data were downloaded for (1) the nearest grid cell to the study site, (2) the two IPCC scenarios of greenhouse gas emission A2 and B2 and (3) simulated by the five following models: HIRHAM (two different model runs available from the Danish as well as the Norwegian Meteorological institutes), PROMES (Universidad Complutense de Madrid), RCAO (Swedish Meteorological and Hydrological Institute), HadRM3P (Hadley Centre for Climate Prediction and Research) and RegCM (Abdus Salam International Centre for Theoretical Physics of Weather and Climate Section). Information about the different models is available in the final report of the PRUDENCE project, where further references are also given (Christensen 2005).

The observed data series of precipitation, incoming longwave radiation and temperature were modified to represent climatic conditions towards the end of the 21st century, largely by following the methods described in Lopez-Moreno et al. (2008) and Bavay et al. (2009). An outline of the methodology is given below.

First, the daily precipitations simulated for each of the six different RCM runs were pooled into 12×3 classes according to 12 months and 3 projections (current conditions, scenarios A2 and B2) (Figure 2, step 1). Second, within each of these 216 classes the values were subdivided into decile ranges (i.e. the lowest, second-lowest, …, highest 10% percent of data) and the mean of all values within each decile (decile mean range or DMR) was derived (Figure 2, step 2). Third, the separate DRM values were averaged over the six RCM runs (Figure 2, step 3). Fourth, the difference between the two future scenarios and the current conditions was described by dividing the DRM values for each scenario by the respective values of the reference simulations. This procedure finally results in 10 DRM quotients per 12 months per 2 scenarios (Figure 2, last step).

To generate model input data for the two scenarios, the measured data were manipulated using these DRM quotients. The measured precipitation data were pooled into monthly classes. For each of these 12 classes, the DRM values were calculated and each measured value was also assigned to its specific decile range. This allowed each measured precipitation value to be manipulated by multiplying it with its month-, deciles range- and scenario-specific DRM quotient (Figure 3, left panel). To modify the incoming longwave radiation measurements, the same method was applied as for precipitation but with two exceptions. First, the DRM values of daily averages were determined instead of daily sums. Second, the effect of
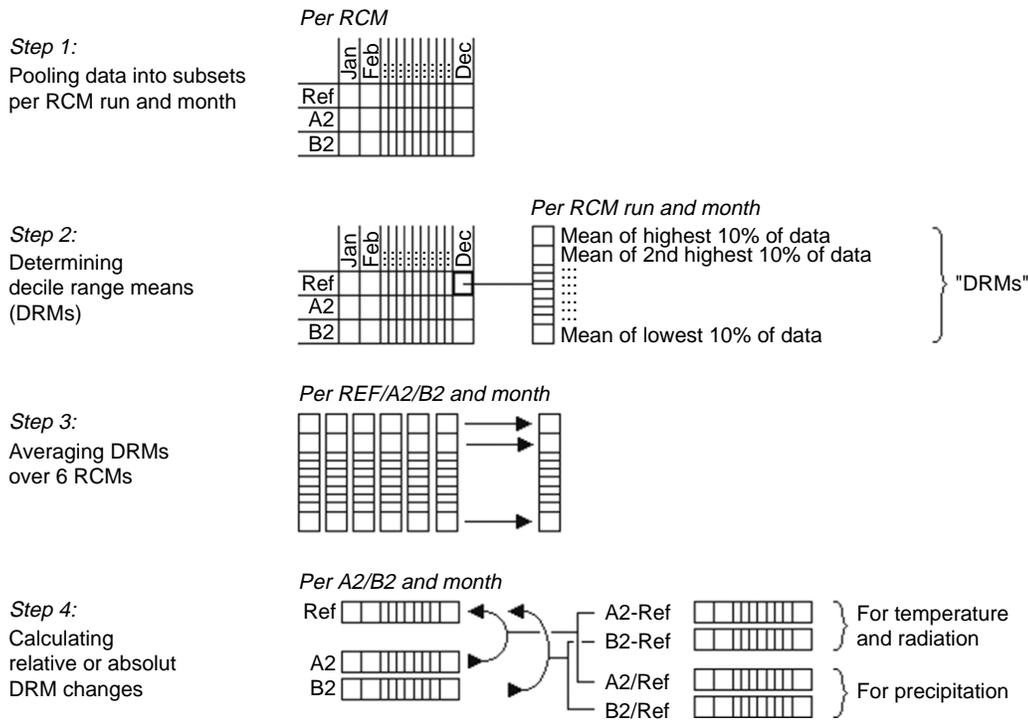
Figure 2 | Flowchart illustrating the statistical downscaling procedure adopted from Bavay *et al.* (2009).

climate change was described with differences instead of quotients between the two future scenarios and the current conditions (Figure 3, right panel).

As temperature exhibits a daily cycle, the above-described methodology was extended to account for the change in daily temperature range also. Therefore, the highest and lowest daily temperatures were modified separately (Figure 4). Finally, the hourly temperatures

between the modified daily maximum and minimum values were determined in two steps. First, for both the originally observed as well as the already changed daily extreme values, a linear change was assumed for the temperatures lying between observations. Second, the differences between these two curves were added to the observed record of hourly temperatures. Note that this modification does not deform the altitudinal gradients as observed for the present conditions.
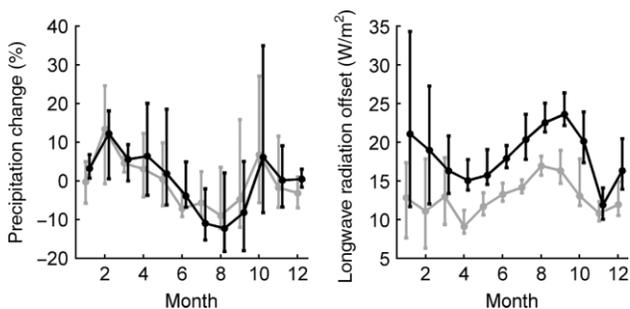

Figure 3 | Change in precipitation (left panel) and incoming longwave radiation (right panel) due to climate warming for scenario A2 (black line) and scenario B2 (grey line). The line shows the change between the control period and the two emission scenarios for the fifth decile for each month in the year. The bars shows the corresponding change for the first and the tenth deciles.

RESULTS

Validation of reference simulation

The modelled snow depths for the reference simulation were compared against independent measurements of snow depth (Figure 5). Measurements were only available from outside the basin. The five measurement stations were located on flat fields 5–15 km away from the basin, ranging in elevation from 1,440 to 2,430 m a s l. and only available after 1998. The measured snow depths were interpolated to
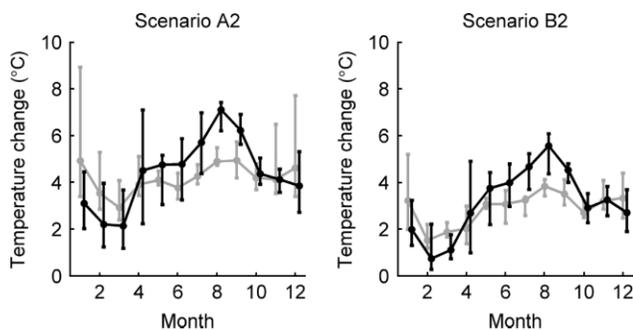
Figure 4 | Change in maximum (black line) and minimum (grey line) temperatures for scenario A2 (left panel) and B2 (right panel). The line shows the change between the control period and the two emission scenarios for the fifth decile for each month in the year, and the bars shows the corresponding change for the first and the tenth deciles.

the same grid (100 m resolution) as used for the Alpine3D simulations applying the interpolation methods from Zappa *et al.* (2005). The average snow depth for all grid cells of flat pixels (slope angle less than 15°) between 2,000 m and 2,500 m elevation were compared because the interpolation is only able to reproduce snow depths in regions of similar terrain (i.e. flat fields) and of similar altitudes as the stations. The comparison shows good agreement between modelled and interpolated snow depths. The simulation represents dynamic changes well, but underestimates the peak snow depths for the first winter and overestimates the snow depths of the 2004/05 and 2005/06 winters.

Climate change characteristics

Predicted changes in precipitation show a strong seasonal pattern (Figure 3, left panel). Winter precipitation is expected to increase by up to 14% in February. In summer, however, the climate models simulate a reduction in precipitation by around 12% in July and August. Both
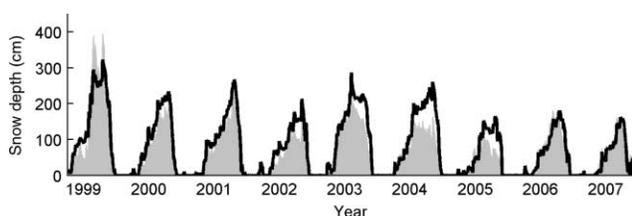
emission scenarios provide similar precipitation estimates. For longwave radiation, on the other hand, an increase throughout the whole year is predicted with significant differences between the scenarios (Figure 3, right panel). The offsets lie between 11 and 24 W/m^2 for scenario A2 and between 9 and 17 W/m^2 for scenario B2. As expected, they correlate to the temperature increase which varies differently throughout the year for the daily highest and lowest temperatures (Figure 4). In August, the increase in the maximum temperatures (7°C for scenario A2 and 5°C according to scenario B2) are greater than for the lowest temperatures. In winter, on the contrary, the increase in minimum temperatures (5°C for scenario A2 and 3°C for scenario B2) is higher than for maximum temperatures. The monthly spread in temperature therefore increases for the summer, whereas it decreases during winter.

Snow-covered area and average water equivalent of snow

Today, the whole basin is snow covered from the end of November until the end of May (Figure 6). Even in summer, 14% of the catchment remains snow covered and contributes to glacier accumulation. The peak in average snow water equivalent of 630 mm occurs during the first part of May. The accumulation period starts at the beginning of October and the ablation period ends in late August. For scenario A2, the catchment is completely snow covered from the end of December until mid-April. The predicted snow season therefore begins almost one month later and ends at least one month earlier than today. For scenario B2, the corresponding snow-covered season lasts from mid-December until the beginning of May.
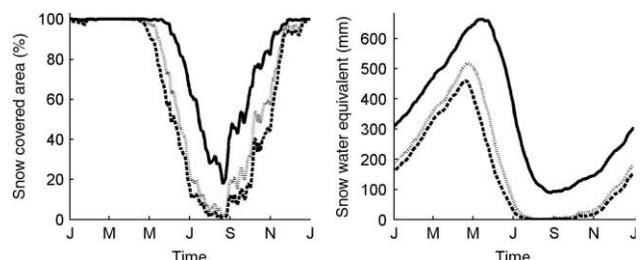

Figure 5 | Modelled snow depths (filled line) and interpolated snow depths (grey area) averaged over the flatter regions of the basin (slope angle less than 15°) between 2,000 and 2,500 m elevation.

Figure 6 | The effect of climate change on snow covered area (left panel) and on the average snow water equivalent (right panel). Current conditions (filled line), scenario A2 (dashed line) and scenario B2 (dotted line).

In summer, the basin will be snow free under both emission scenarios. For scenario A2, the predicted highest snow water equivalent occurs in the later half of April and is 27% lower than today. The timing of the highest snow water equivalent is similar for scenario B2, which decreases by 18% compared to present conditions. The accumulation period starts at the beginning of October and the ablation period ends at the beginning of July for both emission scenarios. The predicted accumulation of snow seems to accelerate slightly while, according to these results, the predicted melting rate will be slower than under current climatic conditions.

Variation of snow distribution with altitude

The peak snow water equivalents throughout the year increase with altitude because lower temperatures at the uppermost part of the basin allow a longer snow accumulation period (Figure 7). Under present climatic conditions, the highest snow water equivalent varies from 640 to 1,925 mm depending on altitude. Almost no snow melts above elevations of 3,300 m, resulting in peak snow water equivalents near the total yearly precipitation. For scenario A2, the highest snow water equivalents vary from 365 to 670 mm depending on altitude. For the less pronounced scenario B2, the values are slightly higher (from 460 to 720 mm). The changes in volume water stored as snow depend on the area distribution over the altitudes in the watershed and the peak snow water equivalents. Today, most water is stored as snow on the central and highest elevations with volumes between 0.84 and 0.94 million m^3 of water. Here, the greatest decreases are also simulated in

the case of a warming climate. The volumes decrease on the middle altitudes with 0.18 million m^3 of water and on the higher elevations with 0.51 million m^3 of water.

Duration of a seasonal snow cover for different altitudes

As expected, the duration of seasonal snow cover is longer at higher altitudes because of the negative temperature gradient with elevation (Figure 8). Today, the snow season starts at altitudes just below 2,800 m early in October and on the lowest elevations of the basin at the beginning of November. The snow season ends in mid-July just below 2,800 m and at the beginning of June for the lowest parts. Above 2,800 m, the snow pack lasts the whole summer during some of the years within the simulation period. There is therefore no well-defined period with a seasonal snow cover.

On the high elevations, the snow contributes to glacier accumulation. For scenario A2, the snow season is expected to start in late November at low elevations and in mid-October for the highest areas of the basin. The snow season starts about one month later than today. The snow season also ends earlier in the future according to these simulations, between the beginning of May and the end of July; this is around one and a half months earlier than today. The predicted changes are not as drastic for scenario B2, where the snow season starts between mid-November and the beginning of October. For both future scenarios, the snow cover in the basin is simulated to complete melt-out leaving no zones for glacier accumulation. The highest snow
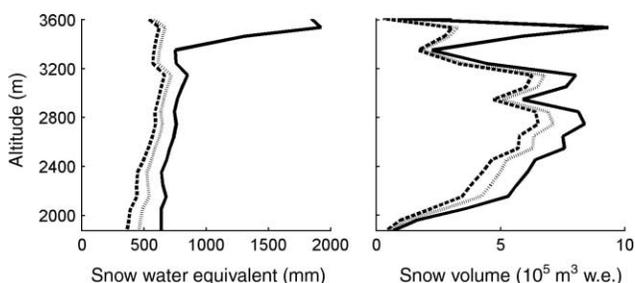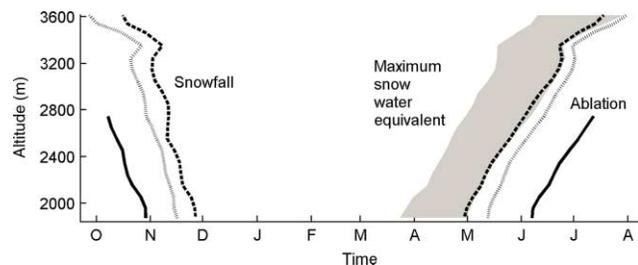

Figure 7 │ The effect of climate change on maximal snow water equivalent (left panel) and total volume of water equivalent (right panel) against altitude. Current conditions (filled line), scenario A2 (dashed line) and scenario B2 (dotted line).

Figure 8 │ The elevation dependence of the first snowfall that builds a continuous snow cover until ablation and the shift in timing of highest snow water equivalent towards winter from spring. Current conditions (filled line), scenario A2 (dashed line), scenario B2 (dotted line) and shift in maximum snow water equivalent from current conditions to scenario A2 (shaded area).

accumulation, which occurs as the snow water equivalent reaches its maximum, is simulated to occur one month earlier than the reference simulation.

DISCUSSION AND CONCLUSIONS

Simulations of the snow-cover response to changes in climate have been presented. The study site represents a typical watershed on higher altitudes, and is covered by a glacier to half its extent. The glacier is evidence of cold temperatures and high precipitation rates over the past. The reference and the prognostic simulations cover time periods providing estimates of the conditions of today and at the end of the 21st century.

Snow-cover models using a degree-day factor approach can efficiently simulate the spatial and temporal distribution of a snow cover when carefully calibrated (Zappa *et al.* 2003). However, such methods may not be appropriate for climate change studies. The assumption of stationary calibration parameters may not be valid if entering new climatic conditions outside of the calibration range. This is likely to be the case as climate model projections predict an acceleration of global warming in the 21st century (IPCC 2007). In contrast, models describing internal snow processes and simulating the surface albedo according to snow grain types seem more capable of representing the energy budget of the snow pack under varying meteorological conditions (Etchevers *et al.* 2004). This makes them more suitable for estimating trends in the snow pack response to climate change. Alpine3D resolves these processes, the snow grain development within each layer of the snow pack and its influence on the surface albedo, as well as the interactions of the surrounding terrain on the radiation budget. The heat fluxes at the lower boundary between the snow pack and the ground are also taken into account. The effect of a glacier beneath the seasonal snow cover is therefore modelled well.

However, even with an appropriate snow model considerable limitations remain. Part of the uncertainty in the model results may arise from inconsistencies between the RCM projections and the observed meteorological records. Single RCM simulations were shown to reproduce observed temperatures with a bias of less than 2°C and simulated precipitation amounts to compare to observations within 10–20% for the Alps (Giorgi *et al.* 2004). Deque *et al.* (2005) concluded that trust in RCM estimates of precipitation can only be achieved by an ensemble of model runs, as was the case with the PRUDENCE project.

Indeed, a follow-up study stated that the simulated climate change signal from the PRUDENCE ensemble is significant compared to the uncertainties between the models (Deque *et al.* 2007). In this study, the PRUDENCE model simulations were applied by evaluating the differences between control and scenario runs. This delta-change approach is less sensitive to problems that may arise if the control run is not perfectly representative of local observations (Raisanen 2008).

The interpolation of the meteorological measurements to gridded model input data may also introduce uncertainties in the results. Interpolating techniques cannot represent small-scale processes and local phenomena, such as catabatic winds from glaciers or effects due to persistent cloud patterns, with certainty. However, such techniques project the main pattern of spatial and temporal variability (such as temperature lapse rates) at a level of complexity that allows reasonable seasonal snow distribution model results. Using interpolated meteorological fields as input to snow models has previously been shown to give accurate estimates of snow-cover distributions and discharges in mountainous terrain (Lehning *et al.* 2006; Michlmayr *et al.* 2007; Bavay *et al.* 2009; Hirashima *et al.* 2008).

Also in this study, the reference simulation reproduces the snow cover reasonably well within the watershed (Figure 5). A further shortcoming relates to the parameterization of longwave radiation, which is typically site-specific. Here, transferability problems may introduce inaccuracies of the modelled snowmelt rates. However, the method used here was shown to accurately reproduce longwave radiation for different sites (Pirazzini *et al.* 2000; Michlmayr *et al.* 2007) and, in this study, the snowmelt rates simulated for the current conditions compared well with the observations. Finally, the redistribution of snow from wind and avalanches is important and influences the amount of snow on some grid points. The effects over those regions that have been averaged in this study are assumed to be minor.

The simulations show drastic changes in both the temporal and spatial patterns of the snow cover in the basin. The snow season shortens by one month at the beginning of the winter and by between one to two months at the end of the winter, compared to the conditions of today. Similar decreases in snow season duration in Switzerland have been modelled in previous studies (Beniston *et al.* 2003b; Jasper *et al.* 2004). The predicted decrease in days with snow cover is not as severe as on lower altitudes, where the average winter temperatures oscillate around zero (Hantel & Hirtl-Wielke 2007). The combined effect of higher temperatures and longer snow-free periods induces higher evaporation rates during summer and lower accumulated sublimation during winter (Dankers & Christensen 2005). A shift in timing and a decrease in runoff can therefore be expected.

Further, in the studied basin the most marked impacts of climate warming on the snow pack will occur in the uppermost parts of the basin. At these locations, a predicted increase in temperature would lead to a total ablation of snow; consequently, the present accumulation area of the glacier would no longer exist. However, the predicted winter temperatures will still fall below zero at these high altitudes, allowing a significant snow accumulation. The predicted increases in precipitation during the first winter months seem to accelerate the snow accumulation rates compared to the reference simulation.

On the other hand, the melt rate of the snow pack seems to decelerate according to the prognostic simulations compared to the conditions of today. This could arise because the incident solar radiation is lower during the ablation period that occurs about one month earlier than today. As a simple validation of the simulations, the elevation profiles for the highest snow water equivalent are to be shifted upwards by about 500 m to match the current conditions. This corresponds to an increase in temperature of about 3.5°C assuming a vertical temperature lapse rate of 0.7°C, which is between the mean annual temperature increase expected towards the end of the 21st century for scenarios A2 and B2 (Figure 4).

This study extends the earlier findings of a decline in snow cover due to climate change to the higher regions of the Alps in Switzerland. With a reduced snow cover, further glacier retreat and soil development, the hydrological response of the type of watershed studied may change. Further studies are therefore important.

REFERENCES

Barnett, T. P., Adam, J. C. & Lettenmaier, D. P. 2005 Potential impacts of a warming climate on water availability in snow-dominated regions. *Nature* **438**, 303–309.

Bavay, M., Lehning, M., Jonas, T. & Löwe, H. 2009 Simulations of future snow cover and discharge in alpine headwater catchments. *Hydrol. Process.* **23**, 95–108.

Beniston, M. 1997 Variations of snow depth and duration in the Swiss Alps over the last 50 years: links to changes in large-scale climatic forcings. *Clim. Change* **36**, 281–300.

Beniston, M., Keller, F. & Goyette, S. 2003a Snow pack in the Swiss Alps under changing climatic conditions: an empirical approach for climate impacts studies. *Theor. Appl. Climatol.* **74**, 19–31.

Beniston, M., Keller, F., Koffi, B. & Goyette, S. 2003b Estimates of snow accumulation and volume in the Swiss Alps under changing climatic conditions. *Theor. Appl. Climatol.* **76**, 125–140.

Bultot, F., Gellens, D., Schadler, B. & Spreafico, M. 1994 Effects of climate-change on snow accumulation and melting in the Broye catchment (Switzerland). *Clim. Change* **28**, 339–363.

Christensen, J. H. 2005 *Prediction of Regional scenarios and Uncertainties for Defining European Climate change risks and Effects*. PRUDENCE final report. Copenhagen. Denmark.

Christensen, J. H., Carter, T. R., Rummukainen, M. & Amanatidis, G. 2007 Evaluating the performance and utility of regional climate models: the PRUDENCE project. *Clim. Change* **81**, 1–6.

Dankers, R. & Christensen, O. B. 2005 Climate change impact on snow coverage, evaporation and river discharge in the sub-arctic Tana Basin, Northern Fennoscandia. *Clim. Change* **69**, 367–392.

Deque, M., Jones, R. G., Wild, M., Giorgi, F., Christensen, J. H., Hassell, D. C., Vidale, P. L., Rockel, B., Jacob, D., Kjellstrom, E., de Castro, M., Kucharski, F. & van den Hurk, B. 2005 Global high resolution versus Limited Area Model climate change projections over Europe: quantifying confidence level from PRUDENCE results. *Clim. Dyn.* **25**, 653–670.

Deque, M., Rowell, D. P., Luthi, D., Giorgi, F., Christensen, J. H., Rockel, B., Jacob, D., Kjellstrom, E., de Castro, M. & van den Hurk, B. 2007 An intercomparison of regional climate simulations for Europe: assessing uncertainties in model projections. *Clim. Change* **81**, 53–70.

Etchevers, P., Golaz, C., Habets, F. & Noilhan, J. 2002 Impact of a climate change on the Rhone river catchment hydrology. *J. Geophys. Res. Atmos.* **107**(D16), 4293.

Etchevers, P., Martin, E., Brown, R., Fierz, C., Lejeune, Y., Bazile, E., Boone, A., Dai, Y., Essery, R., Fernandez, A., Gusev, Y., Jordan, R., Koren, V., Kowalcyzk, E., Nasonova, N. O., Pyles, R. D., Schlosser, A., Shmakin, A. B., Smirnova, T. G., Strasser, U., Verseghy, D., Yamazaki, T. & Yang, Z. L. 2004 Validation of the energy budget of an alpine snowpack simulated by several snow models (SnowMIP project). *Ann. Glaciol.* **38**, 150–158.

Fierz, C., Riber, P., Adams, E. E., Curran, A. R., Fohn, P. M. B., Lehning, M. & Pluss, C. 2003 Evaluation of snow-surface energy balance models in alpine terrain. *J. Hydrol.* **282**, 76–94.

Gellens, D., Barbieux, K., Schadler, B., Roulin, E., Aschwanden, H. & Gellens-Meulenberghs, F. 2000 Snow cover modelling as a tool for climate change assessment in a Swiss Alpine catchment. *Nordic Hydrol.* **31**, 73–88.

Giorgi, F., Bi, X. & Pal, J. S. 2004 Mean, interannual variability and trends in a regional climate change experiment over Europe. I. Present-day climate (1961–1990). *Clim. Dyn.* **22**, 733–756.

Hammerli, A., Waldhuber, S., Miniaci, C., Zeyer, J. & Bunge, M. 2007 Local expansion and selection of soil bacteria in a glacier forefield. *Eur. J. Soil Sci.* **58**, 1437–1445.

Hantel, M. & Hirtl-Wielke, L. M. 2007 Sensitivity of alpine snow cover to European temperature. *Int. J. Climatol.* **27**, 1265–1275.

Hirashima, H., Nishimura, K., Yamaguchi, S., Sato, A. & Lehning, M. 2008 Avalanche forecasting in a heavy snowfall area using the snowpack model. *Cold Reg. Sci. Technol.* **51**, 191–203.

Horton, P., Schaefli, B., Mezghani, A., Hingray, B. & Musy, A. 2006 Assessment of climate-change impacts on alpine discharge regimes with climate model uncertainty. *Hydrol. Process.* **20**, 2091–2109.

Hosaka, M., Nohara, D. & Kitoh, A. 2005 Changes in snow cover and snow water equivalent due to global warming simulated by a 20 km-mesh global atmospheric model. *SOLA* **1**, 93–96.

Huss, M., Farinotti, D., Bauder, A. & Funk, M. 2007 *Modelling Runoff from Highly Glacierized Alpine Drainage Basins in a Changing Climate*. Workshop on Glaciers in Watershed and Global Hydrology, Obergurgl, Austria, pp. 3888–3902.

IPCC 2007 *Climate Change 2007 – The Physical Science Basis*. Cambridge University Press, Cambridge.

Jasper, K., Calanca, P., Gyalistras, D. & Fuhrer, J. 2004 Differential impacts of climate change on the hydrology of two alpine river basins. *Clim. Res.* **26**, 113–129.

Keller, F., Goyette, S. & Beniston, M. 2005 Sensitivity analysis of snow cover to climate change scenarios and their impact on plant habitats in alpine terrain. *Clim. Change* **72**, 299–319.

Laternser, M. & Schneebeli, M. 2003 Long-term snow climate trends of the Swiss Alps (1931–99). *Int. J. Climatol.* **23**, 733–750.

Lehning, M., Bartelt, P., Brown, B., Fierz, C. & Satyawali, P. 2002 A physical SNOWPACK model for the Swiss avalanche warning Part II: Snow microstructure. *Cold Reg. Sci. Technol.* **35**, 147–167.

Lehning, M., Volksch, I., Gustafsson, D., Nguyen, T. A., Stahli, M. & Zappa, M. 2006 ALPINE3D: a detailed model of mountain surface processes and its application to snow hydrology. *Hydrol. Process.* **20**, 2111–2128.

Lopez-Moreno, J. I., Goyette, S., Beniston, M. & Alvera, B. 2008 Sensitivity of the snow energy balance to climatic changes: prediction of snowpack in the Pyrenees in the 21st century. *Clim. Res.* **36**, 203–217.

Marty, C. 2008 Regime shift of snow days in Switzerland. *Geophys. Res. Lett.* **35**, L12501.

Michlmayr, G., Lehning, M., Koboltschnig, G., Holzmann, H., Zappa, M., Mott, R. & Schoner, W. 2007 *Application of the Alpine 3D Model for Glacier Mass Balance and Glacier Runoff Studies at Goldbergkees*. Austria Workshop on Glaciers in Watershed and Global Hydrology, Obergurgl, Austria, pp. 3941–3949.

Middelkoop, H., Daamen, K., Gellens, D., Grabs, W., Kwadijk, J. C. J., Lang, H., Parmet, B., Schadler, B., Schulla, J. & Wilke, K. 2001 Impact of climate change on hydrological regimes and water resources management in the rhine basin. *Clim. Change* **49**, 105–128.

Nakicenovic, N., Grübler, A. & McDonalds, A. 1998 *Global Energy Perspectives*. Cambridge University Press, Cambridge.

Obleitner, F. & Lehning, M. 2004 Measurement and simulation of snow and superimposed ice at the Kongsvegen glacier, Svalbard (Spitzbergen). *J. Geophys. Res.* **109**, D04106.

Pirazzini, R., Nardino, M., Orsini, A., Calzolari, F., Georgiadis, T. & Levizzani, V. 2000 Parameterization of the downward longwave radiation from clear and clouded skies at Ny Alesund (Svalbard), IRS 2000. In: Smith, W. L. & Timofeyev, Y. M. A. (eds) *Current Problems in Atmospheric Radiation*. Deepack Publishing, Hampton, Virginia, pp. 559–562.

Raisanen, J. 2008 Warmer climate: less or more snow? *Clim. Dyn.* **30**, 307–319.

Rasmus, S., Raisanen, J. & Lehning, M. 2004 Estimating snow conditions in Finland in the late 21st century using the SNOWPACK model with regional climate scenario data as input. *Ann. Glaciol.* **38**, 238–244.

Schaefli, B., Hingray, B. & Musy, A. 2007 Climate change and hydropower production in the Swiss Alps: quantification of potential impacts and related modelling uncertainties. *Hydrol. Earth Syst. Sci.* **11**, 1191–1205.

Scherrer, S. C. & Appenzeller, C. 2006 Swiss Alpine snow pack variability: major patterns and links to local climate and large-scale flow. *Clim. Res.* **32**, 187–199.

Scherrer, S. C., Appenzeller, C. & Laternser, M. 2004 Trends in Swiss Alpine snow days: the role of local- and large-scale climate variability. *Geophys. Res. Lett.* **31**, L13215.

Shabalova, M. V., van Deursen, W. P. A. & Buishand, T. A. 2003 Assessing future discharge of the river Rhine using regional climate model integrations and a hydrological model. *Clim. Res.* **23**, 233–246.

Shepard, D. 1968 A two-dimensional interpolation function for irregularly-spaced data. In: *Proceedings of the 1968 ACM National Conference*, pp. 517–524.

Swift, D. A., Nienow, P. W., Hoey, T. B. & Mair, D. W. F. 2005 Seasonal evolution of runoff from Haut Glacier d'Arolla, Switzerland and implications for glacial geomorphic processes. *J. Hydrol.* **309**, 133–148.

Wielke, L. M., Haimberger, L. & Hantel, M. 2004 Snow cover duration in Switzerland compared to Austria. *Meteorologische Zeitschrift* **13**, 13–17.

Zappa, M., Pos, F., Strasser, U., Warmerdam, P. & Gurtz, J. 2003 Seasonal water balance of an Alpine catchment as evaluated by different methods for spatially distributed snowmelt modelling. *Nordic Hydrol.* **34**, 179–202.

Zappa, M., Song, Z. H., Baumgartner, M. F., Gurtz, J. & Schaedler, B. 2005 The Changjiang flood forecasting assistance project. *Proceedings of the International Conference on Headwater Control VI: Hydrology*, Ecology and Water Resources in Headwaters, Bergen, Norway.

Zemp, M., Haeberli, W., Hoelzle, M. & Paul, F. 2006 Alpine glaciers to disappear within decades? *Geophys. Res. Lett.* **33**, L13504.